Dual-Band 4G Eyewear Antenna and SAR Implications

Aykut Cihangir, Chinthana J. Panagamuwa, Will G. Whittow, Gilles Jacquemod, Frédéric Gianesello, Romain Pilard, Cyril Luxey

***Abstract*— This paper presents low-cost and easy-to-manufacture dual-band antenna solution to achieve cellular 4G (LTE-Advanced) coverage in smart eyewear devices. Coupling element type antenna has been evaluated with appropriate matching networks to cover the target bands of 700-960MHz and 1.7-2.7GHz. To emulate a realistic device, an ABS plastic dielectric frame has been designed and manufactured using 3D printing technology. Simulations for the antenna are carried out in three typical use-case scenarios which are "with user's head", "with head and hand" and "free space". The simulations are validated through S-parameters, efficiency and radiation pattern measurements using fabricated frame and antenna prototype in the presence of head and hand phantoms. The SAR behavior of the antenna designs is also investigated through simulations and measurements. It is demonstrated that SAR values are found to be above the limitations which might be problematic in practical use if the transmit power of the eyewear is not reduced.**

***Index Terms*—smart eyewear, antenna, coupling element, matching network, 4G, LTE, cellular network, SAR**

I. Introduction

The wireless cellular communication standards have undergone several improvements since the launch of the first analog systems. Recently, with the introduction of smartphones, a continuous necessity to provide higher data rates to the users has arisen. For this reason, LTE-Advanced standard was introduced as the fourth generation of wireless cellular communications.

A parallel avenue of research that has seen an explosion of activity in recent years is body-centric communications that involve transmission between on-body and off-body antennas. As an interesting and hot recent topic, there are a number of smart eyewear devices already available in the market or being prepared for imminent release [1-5]. The common properties of all these eyewear systems are: a lens-reflector screen in front of the user's eye, a touchpad on the side of the eyewear to adjust the settings or use the applications, a speaker/microphone pair and a Wi-Fi/Bluetooth transceiver. The devices have a wide variety of application areas including navigation, video capture and streams, accept/reject calls from a paired mobile phone.

Manuscript received February 2016.

A. Cihangir, C. Luxey and Gilles Jacquemod are with EpOC, Université Nice Sophia Antipolis, Valbonne, France (phone: +33-(0)4-93-95-51-88; fax: +33-(0)4-93-95-51-89; e-mail: cyril.luxey@unice.fr)

C. Luxey is also with Institut Universitaire de France (IUF), Paris, France.

F. Gianesello, R. Pilard are with STMicroelectronics, Crolles, France.

C. Panagamuwa and W. Whittow are with the Wireless Communications Research Group, School of Electronic, Electrical and Systems Engineering, Loughborough University, Loughborough LE11 3TU, U.K. (e-mail: w.g.whittow@lboro.ac.uk; C.J.Panagamuwa@lboro.ac.uk).

However, the wireless connectivity of these devices is currently limited to Wi-Fi 802.11b/g and Bluetooth where the eyewear connects either to a hotspot, a set-top box or a peripheral smartphone. The antenna is generally placed behind the user's ear like in a wireless headset configuration. The Specific Absorption Rate (SAR) is not a concern due to the low output power levels of WLAN and Bluetooth standards. It is foreseen that these eyewear devices might partially act as smartphones in the future which creates the necessity to make them suitable to communicate with 4G cellular networks. Such devices would offer significantly higher data rates compared to Bluetooth and pave the way for a new wave of functionality. From the antenna design perspective, this requires some dual-band antennas to cover 700-960MHz for the low-band (LB) and 1.7-2.7GHz for the high-band (HB). This is extremely challenging considering the very small area that can be allocated to the antenna. As a consequence, an electrically-small antenna is required especially in the LB. To maximize the bandwidth potential (BP) from an electrically small antenna in a mobile terminal, capacitive coupling elements (CE) have been proposed in the literature. The CEs are non-resonant structures which are used to excite the proper wavemodes on the system ground plane of the device [6-7]. By exploiting the low quality factor of the system ground plane, a high BP can be obtained. The antenna is then tuned to the desired bands using a proper matching network (MN) at the antenna feed. Such antenna solutions with their corresponding matching networks can be found in [8-11]. Previously, the authors have conducted a feasibility study to demonstrate that it was possible to use CE antennas to cover 4G frequencies in eyewear devices [12]. It was shown that the target frequency bands could be covered with a reflection coefficient below -6dB, with CEs placed in three different regions of the printed circuit board (PCB). The feasibility study included only simulation results of the antennas, without any fabrication or measurement. Taking [12] as the starting point, both the CE and the MN are re-designed in this paper in order to obtain a real manufactured prototype as realistic as possible. A realistic ABS plastic eyewear frame was designed and fabricated using 3D printing technology. Suitable realistic CE type antenna structure with the corresponding MN was optimized and integrated into this eyewear frame to operate in the 700-960MHz LB and the 1.7-2.7GHz HB. It should be noted that in the 4G operating mode the output power level from the front-end module can be significantly higher than Bluetooth devices. So considering an eyewear antenna to operate in 4G cellular networks, specific absorption rate (SAR) becomes an essential parameter to investigate in order to meet international regulations. Section II presents the design and optimization of the manufactured antenna design. A comparison of simulations and measurements of the reflection coefficient, total efficiency and radiation patterns taking into account the user's head is also presented in this section. The effect of the user's hand and the antenna performance in free space is discussed in Section III. SAR simulations and measurements are given in Section IV.

Finally, conclusions are discussed in Section V.

II. Antenna Design

To validate one of the antenna concept presented in [12], a CE with a realistic dielectric frame was designed and manufactured. The simulation setup presented in Fig. 1 was prepared for the antenna design, in the EMPIRE XCcel electromagnetic software [13]. The Specific Anthropomorphic Mannequin (SAM) head [14] was used for simulations and measurements. 3D-printing fast prototyping technology was selected for the fabrication of the eyewear frame using ABS-M30 material. This material is modeled in simulations with an $\varepsilon_r = 2.97$ and $\tan\delta = 0.029$. The parts of the frame on the right side of the head acts as a dielectric casing for the eyewear PCB (casing length is 168mm, height is 19mm and width is 6.8mm). There is a hollow region inside the casing for the placement of the antenna PCB, having a width of 4.8mm, leaving dielectric walls of 1mm thickness on each side (Fig. 2). Although the antenna was optimized for the "with head" condition, two additional use-cases were also evaluated both in simulations and measurements, one being "antenna and frame in free space condition" and the other being "with the user's hand" (Fig. 2) emulating the user using the touchpad. For the electrical properties of the homogeneous tissue, the liquid properties at 1450MHz were used in simulations, to be a mid-value of the target band. The corresponding properties are: ε_r=40.5 and $\tan\delta$ =0.367.

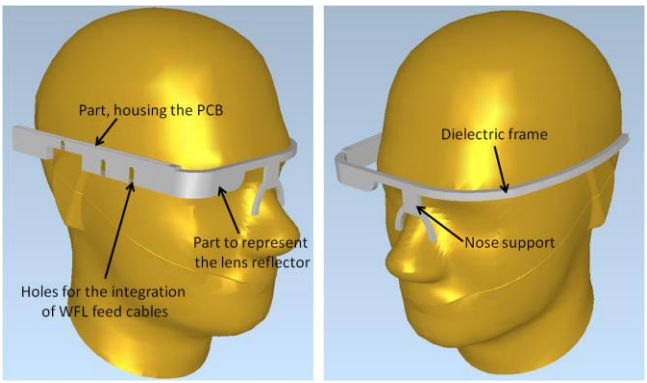

Fig. 1. Optimized eyewear frame on the SAM head

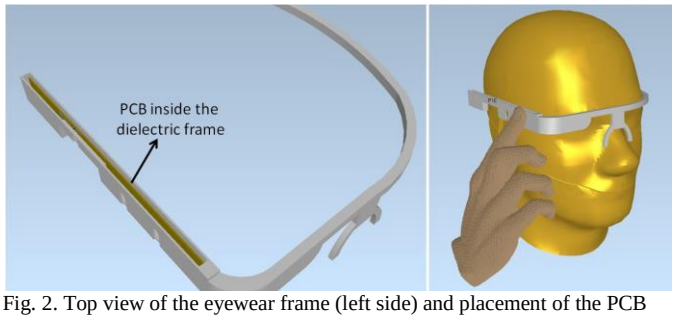

Fig. 2. Top view of the eyewear frame (left side) and placement of the PCB inside the frame. Position of user's hand and fingers (right side).

The CE is printed on one side of a 0.8mm thick FR4 PCB ($\varepsilon_r = 4.4$ and $\tan\delta = 0.02$). The other side of the PCB is used as the ground plane. The location of the CE is towards the end of the PCB, close to the eye. It was hypothesized that the efficiency will be higher in this configuration since the CE is situated further away from the lossy head tissues due to the curved geometry of the head and the straight geometry of the frame. The T-shaped CE geometry can be observed in Fig. 3.

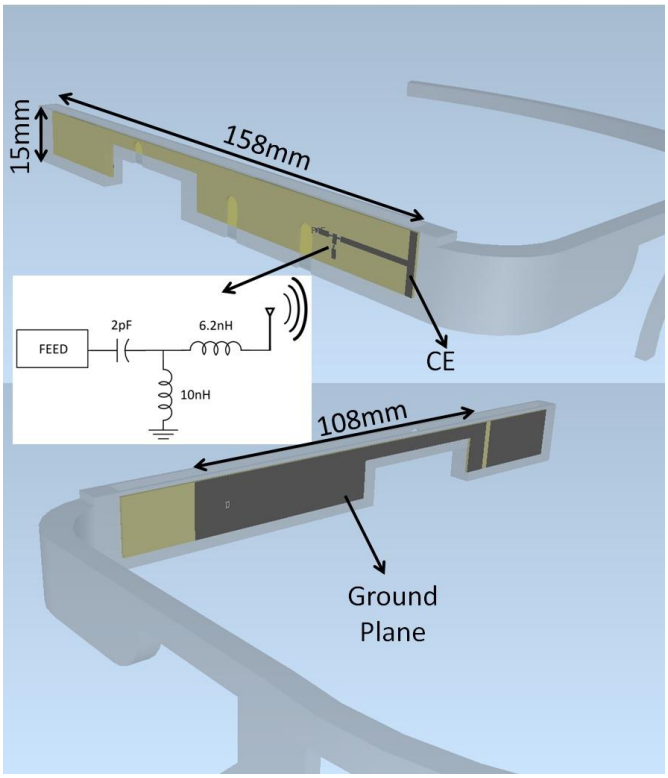

Fig. 3. Model of Antenna Design and its matching network

The ground plane is printed on the inner side of the FR4 PCB. The CE and the MN are situated on the outer side, together with the WFL connector that will be used to feed the antenna. The simulated and measured reflection coefficients of this antenna are presented in Fig. 4. The agreement between simulation and measurement is good except above 2.2GHz. This is thought to be due to the frequency dependent characteristics of the head liquid, which was used as a constant value through the whole simulated frequencies. The antenna can indeed cover the target-band with dual-band behavior with a reflection coefficient below -6dB.

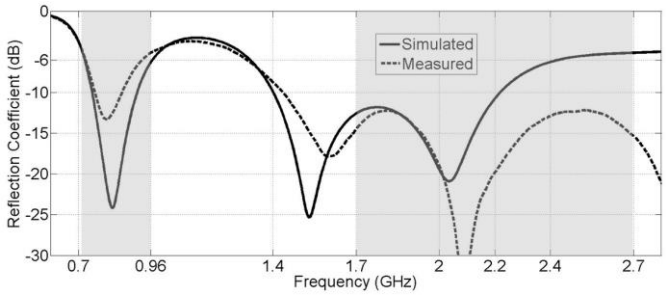

Fig. 4. Simulated and measured reflection coefficient of Antenna Design with frame and 3-element MN on SAM head

Fig. 5 shows the manufactured PCBs used in the measurements. The simulated and measured total efficiency for the general use-case ("with head" configuration) can be seen in Fig. 6. The measured total efficiency ranges from 5 to 9% in the LB and between 18-31% in the HB. The simulated and measured 2D gain patterns of the antenna are compared in Fig. 7, and shows reasonable agreement despite the presence of some ripples.

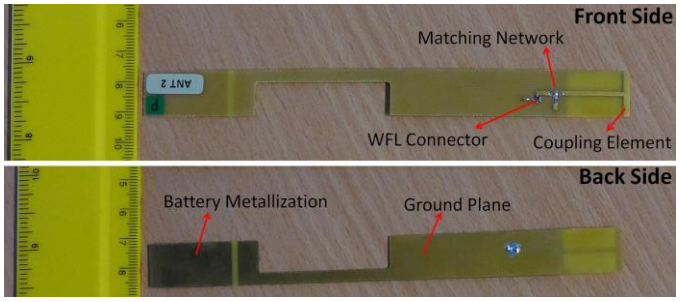

Fig. 5. Manufactured PCBs with Antenna

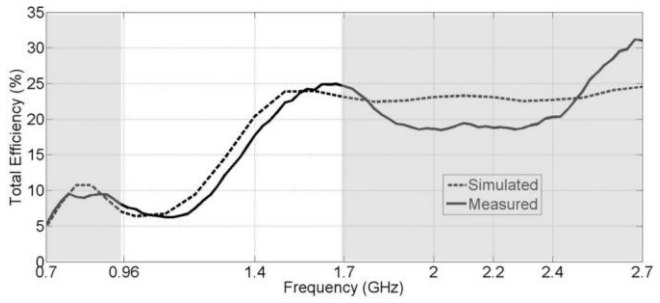

Fig. 6. Simulated and measured total efficiency of Antenna with frame on SAM head

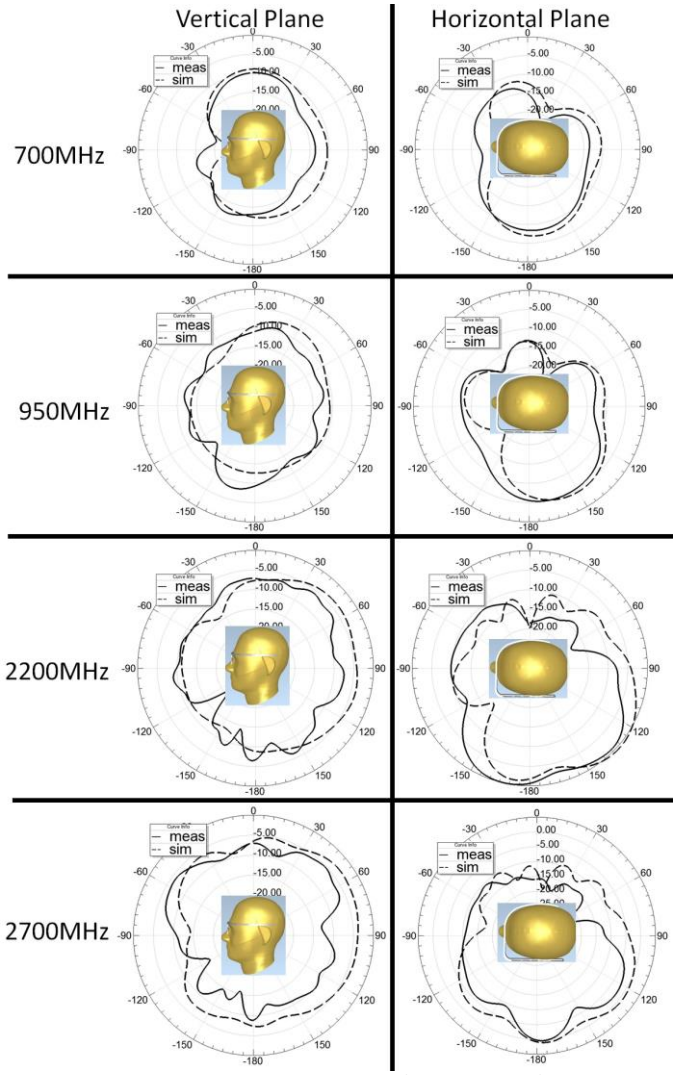

Fig. 7. Measured and simulated gain patterns of Antenna with frame on SAM head (2D cuts)

The radiation is weak in the direction of the head due to losses. The radiation is always maximum in the direction away from the head (in horizontal plane) and splits in several beams as the frequency increases, however, without the creation of any strong deep nulls. The dominant polarization is in the horizontal direction and is superior by as much as 6dB in the LB and 5dB in the HB, compared to vertical polarization (because of the main horizontal currents flowing along the length of the PCB).

Table 1 summarizes the simulated and measured maximum gain values. A fair agreement can be observed between simulations and measurements.

TABLE 1 SIMULATED AND MEASURED MAXIMUM ANTENNA GAIN

	700MHz	950MHz	2200MHz	2700MHz
Simulated	-6.65dBi	-4.42dBi	0.59dBi	1.21dBi
Measured	-8.29dBi	-5.03dBi	0.65dBi	0.52dBi

III. MEASUREMENT IN DIFFERENT USE CASE

As previously mentioned in Section II, three realistic use-cases were targeted for the smart eyewear devices. This section presents the measurements of those three use-cases. The pictures of the measurement setup of different configurations are shown in Fig. 8.

Fig. 8. Measurement configurations for the three targeted use-cases: "free space" using foam spacer (left); "with SAM head" (center) and "with SAM head and phantom hand" (right)

The left figure shows the setup used for "free space" condition where the eyewear is not worn by the user but might need to be operational for incoming calls. The ABS frame with integrated antenna was placed horizontally on a foam support, to keep the antenna leveled in the horizontal plane. The center figure presents the general use-case, "with SAM head" configuration, which was used in the previous measurements in Section II. The right figure shows the set-up for "with SAM head and phantom hand" use-case which emulates the case in which the user uses the touchpad on the side of the device. A positioner placed below the hand was used to keep the hand phantom stable and the finger positioned at the center of the ABS frame. A real human male head configuration was also tested for S-Parameter measurements. The reflection coefficient and total efficiency measurements for the antenna can be found in Fig. 9 and Fig. 10, respectively.

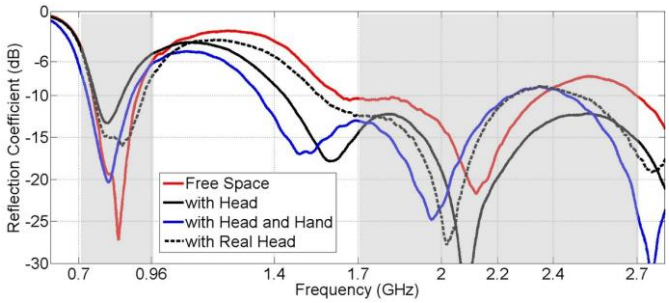

Fig. 9. Measured reflection coefficient for different use case

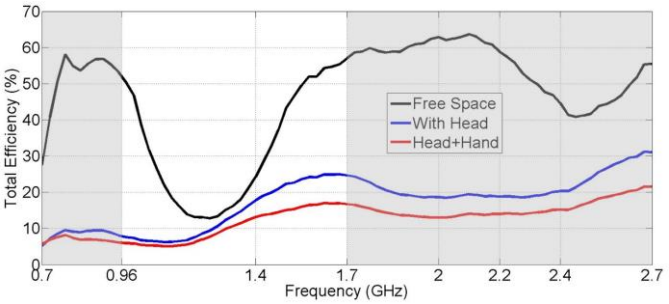

Fig. 10. Measured total efficiency for different use case

As expected, the reflection coefficient performance is slightly worse in free space condition when compared to the "with head" case, because of the lossy nature of the head and also since the MN was fine tuned with the presence of this SAM head. In "with head and hand" case, a slight detuning in the HB can be seen due to the existence of the finger close to the CE. The reflection coefficient measured with a real head is similar compared to the SAM head.

In free space, the efficiency in LB, ranges from 30 to 58%, with a minimum seen around 700MHz mainly because of a poor reflection coefficient at this frequency. In the HB, the free space efficiency varies between 40 and 63%. The total efficiency decrease due to the hand is on average around 5%, with a difference up to 10% in the HB. The total efficiency with the SAM head and hand is ranging from 6 to 8% in the LB and 12 to 21% at the HB. This antenna has a higher efficiency than antennas integrated in typical smartphones (with user's head and hand). Therefore, it demonstrates the suitability of our eyewear device for 4G communications.

IV. SAR Simulations and Measurements

RF Power absorbed by a unit mass of tissue (W/kg) is referred to as SAR and is the internationally recognized dosimetric parameter for testing wireless devices. In Europe, the SAR limit in the head is 2W/kg averaged over 10g for 6 minutes [17]. In the USA, it is 1.6W/kg averaged over 1g for 30 minutes [14]. The 1g and 10g spatially averaged SAR was simulated in EMPIRE XCcel using the SAM head phantom. Measurements were carried out using a Dosimetric and near-field Assessment System (DASY4) [18]. The experimental setup is shown in Fig. 11(a). SAR measurements were taken with continuous wave RF input signals at 900 and 1900MHz. Simulation and measurement result comparisons are shown in Table 2. All results are normalized to 0.25W accepted power after accounting for the port mismatch losses (S_{11}). In all cases, the measured results are lower than their simulation counterparts. Although ferrite beads were used around the RF cable in order to choke any external cable currents, there is still radiation from the cable, as highlighted in the ellipse in Fig. 11(b). As the antenna is placed in close proximity to the head, the SAR levels are sensitive to manufacturing tolerances of the frame. This affects the positioning of the antenna inside the frame, the thickness of the frame as well its dielectric properties. This was verified by carrying out additional measurements with the PCB (without the frame) placed directly against the flat section of the DASY4 twin phantom; these results showed better agreement with simulations. As with all measurement equipments, the DASY4 has a number of parts where measurement uncertainty can be introduced. The three main areas are identified as Measurement equipment (probe), Mechanical Constrains (shell and probe positioning), and Physical parameters (liquid properties). As a result, the worse-case expanded uncertainty budget for the DASY4 quoted in the manufacturer's documentation is ± 21.7% [18].

In all cases, simulated and measured SAR values exceed the international limits. This is partially due to the fact that the total antenna efficiency of the eyewears is double the typical values with generic smartphones with head and hand of the user. In this study, the antenna is also much closer to the phantom head compared to a smartphone that normally rests against the pinna and has the antenna placed on the side of the case away from the head. This is indeed an important finding of this paper which is highly problematic for the safety of the users. Due to the possible placements of an antenna to be integrated in a 4G eyewear, it is believed that it will lead to relatively high efficiency and therefore it will be extremely difficult to comply with the US and European SAR standards. As the total efficiency of the antenna should be large enough for 4G cellular communications, the SAR levels could be reduced by decreasing the transmit power of the front-end module of the eyewear making it operate in a different class mode.

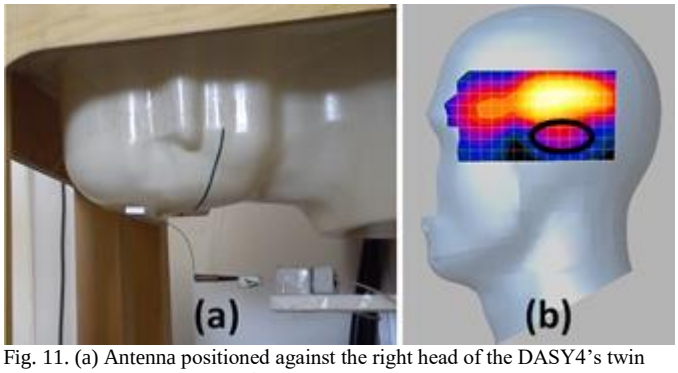

Fig. 11. (a) Antenna positioned against the right head of the DASY4's twin phantom. (b) Visualization of measured SAR area scan at 1900MHz

TABLE 2 SIMULATED AND MEASURED 1G AND 10G SAR (W/KG) FOR ANTENNA. POWER NORMALIZED TO 0.25W ACCEPTED POWER

Frequency (MHz)	Antenna	
	1g SAR	10g SAR
900 (sim.)	4.6	2.6
900 (meas.)	2.9	1.7
1900 (sim.)	8.3	4.1
1900 (meas.)	7.0	3.2

V. Conclusion

An antenna design to cover the 4G cellular communication bands for a smart eyewear device was presented in this paper. A realistic ABS frame which fits the SAM head was designed and manufactured using 3D printing technology. The CE was placed at the end of the PCB, close to the eye and as far as possible from the lossy head tissue. It was shown that this design can achieve dual-band coverage of 700-960MHz and 1.7-2.7GHz with a -6dB reflection coefficient. Considering three possible realistic use-case, S-Parameters and total efficiency measurements were repeated for the antenna design in "free space" and "with head and hand" conditions, showing no significant detuning. The reflection coefficient was also measured in the presence of a real human head. Slight and acceptable differences were encountered between simulations and SAM head phantom measurements.

Finally, SAR simulations and measurements were conducted at 0.9 and 1.9 GHz demonstrating a very important issue about user-antenna interactions. Measured 1g SAR values higher than the US limits for the general public were found at 0.9 and 1.9 GHz. The measured 10g SAR was below the European limits for the general public at 0.9 GHz but above the limit at 1.9 GHz. Note the measured values would be below the limits for all cases for military personnel or trained users in controlled environments where five times higher SAR values are permissible. The high SAR values are largely due to the fact that the total efficiency is double the typical values with generic smartphones with the head and hand. As the total efficiency of the antenna is large enough for cellular communications with 4G networks, the SAR levels could be reduced by decreasing the transmit power of the eyewear devices; making them operate in a different class mode; or adding a series resistor within the RF transmit chain.

Acknowledgment

The authors would like to acknowledge Orange Labs La Turbie and the CIM-PACA design platform. Frederic Devillers from Orange Labs is deeply acknowledged for his valuable help in the mechanical adjustments of the eyewear, phantom head and hand for measurements.

References

[1] "Google Glass," Available at: http://www.google.com/glass/start/
[2] "M100 Smart Glass," Available at: http://www.vuzix.com/UKSITE/consumer/products_m100.html
[3] "RECON Jet," Available at: http://www.reconinstruments.com/products/jet/
[4] "Olympus MEG4.0," Available at: http://www.olympus.co.jp/jp/news/2012b/nr120705meg40j.jsp
[5] "Optinvent ORA," Available at: http://optinvent.com/see-through-glasses-ORA
[6] J. Villanen, J. Ollikainen, O. Kivekas, P. Vainikainen, "Coupling element based mobile terminal antenna structures," IEEE Transactions on Antennas and Propagation, vol.54, no.7, pp. 2142-2153, July 2006.
[7] J. Holopainen, R. Valkonen, O. Kivekas, J. Ilvonen, P. Vainikainen, "Broadband Equivalent Circuit Model for Capacitive Coupling Element–Based Mobile Terminal Antenna," IEEE Antennas and Wireless Propagation Letters, vol. 9, pp. 716-719, 2010.
[8] J. Villanen, C. Icheln, P. Vainikainen, "A coupling element-based quad-band antenna structure for mobile terminals," Microwave and Optical Technology Letters, vol. 49, no. 6, pp. 1277-1282, June 2007.
[9] A. Andujar, J. Anguera, C. Puente, "Ground Plane Boosters as a Compact Antenna Technology for Wireless Handheld Devices," IEEE Trans. on Antennas & Propag., vol. 59, no. 5, pp. 1668-1677, May 2011.
[10] R. Valkonen, J. Ilvonen, P. Vainikainen, "Naturally non-selective handset antennas with good robustness against impedance mistuning," 6th European Conference on Antennas and Propagation 2012 (EuCAP 2012), pp.796-800, 26-30th March 2012.
[11] R. Valkonen, J. Ilvonen, C. Icheln, P. Vainikainen, "Inherently non-resonant multi-band mobile terminal antenna," IET Electronics Letters, vol. 49, no. 1, pp. 11-13, 3rd January 2013.
[12] A. Cihangir, W.G. Whittow, C.J. Panagamuwa, F. Ferrero, G. Jacquemod, F. Gianesello, C. Luxey, "Feasibility Study of 4G Cellular Antennas for Eyewear Communicating Devices," IEEE Antennas and Wireless Propagation Letters, vol. 12, pp. 1704-1707, 2013.
[13] EMPIRE XCcel, Information Available at: http://www.empire.de/
[14] IEEE Std 1528-2003 IEEE Recommended Practice for Determining the Peak Spatial-Average Specific Absorption Rate (SAR) in the Human Head from Wireless Communications Devices: Measurement Techniques
[15] Optenni Lab, Information Available at: http://www.optenni.com/optenni-lab/
[16] Satimo Starlab, Information Available at: http://www.satimo.com/content/products/starlab
[17] Human Exposure to Radio Frequency Fields From Hand-Held and Body-Mounted Wireless Communication Devices-Human Models, Instrumentation, and Procedures—Part 1: Procedure to Determine the Specific Absorption Rate for Hand-Held Devices Used in Close Proximity to the Ear (300 MHz to 3 GHz), IEC 62209-1:2005, 2005.
[18] DASY4 Manual: DASY4 Manual v4.1, Schmid & Partner Engineering AG, March 2003.